Carbohydrate Polymers 116 (2015) 229–236

Contents lists available at ScienceDirect

Carbohydrate Polymers

journal homepage: www.elsevier.com/locate/carbpol

Topical curcumin-loaded hydrogels obtained using galactomannan from *Schizolobium parahybae* and xanthan

Heidegrid Siebert Koop[a], Rilton Alves de Freitas[b], Márcia Maria de Souza[c], Roberto Savi-Jr.[a], Joana Léa Meira Silveira[a,*]

[a] Department of Biochemistry and Molecular Biology, Federal University of Paraná, P.B. 19046, Centro Politécnico, CEP 81531-990 Curitiba, PR, Brazil
[b] Department of Chemistry, Federal University of Paraná, P.B. 19046, Centro Politécnico, CEP 81531-990 Curitiba, PR, Brazil
[c] Postgraduate Program at Pharmaceutical Sciences, University of Vale do Itajaí, Itajaí, Brazil

ARTICLE INFO

Article history:
Received 25 January 2014
Received in revised form 16 July 2014
Accepted 19 July 2014
Available online 29 July 2014

Keywords:
Curcumin
Polysaccharide hydrogel
Galactomannan
Microemulsion
In-vitro skin permeation
Xanthan

ABSTRACT

The curcumin (CUR)-loaded binary hydrogel was formulated using xanthan and galactomannan from *Schizolobium parahybae* (guapuruvu). The binary hydrogels presented gel characteristics, stable pH values and mechanical stress resistance even after 45 days of heat exposure (45 °C). The CUR-loaded hydrogel content was 98.6% for XGMC (xanthan and galactomannan with CUR-microemulsion) after the stability test. The *in vitro* cytotoxicity analysis suggested non-cutaneous membrane irritation, and the *in vitro* skin permeation analysis indicated 2.15 to 2.50 μg mL^{-1} CUR at the stratum corneum, epidermal and dermal levels. The XGEC (xanthan and galactomannan with CUR solubilized in ethanol) and XGMC hydrogels presented 76.8 and 63.2% inhibition of topical inflammation, respectively. Chemical stability and non-cytotoxicity analysis confirm the safety of prolonged exposure of the skin during the topical treatment, offering long-lasting XGEC and XGMC action.

1. Introduction

Mixed polysaccharide systems are used in a wide range of applications because of their ability to interact synergistically (Mannion et al., 1992) and to render materials with controlled properties. In particular, galactomannan blends are used by themselves or in combination with xanthan in a range of applications that include drug delivery (Ughini, Andreazza, Ganter, & Bresolin, 2004; Vendruscolo, Andreazza, Ganter, Ferrero, & Bresolin, 2005). The drug dissolution profile from matrices of galactomannan and xanthan revealed zero order model drug release, indicating their potential as sustained-release vehicles (Ughini et al., 2004). The general structure of seed galactomannans consists of polymeric main-chains of (1 → 4)-linked β-D-mannopyranosyl residues substituted at *O*-6 by single unit side-chains of α-D-galactopyranose. The galactomannan extracted from the seeds of a Brazilian native plant, *Schizolobium parahybae* (Guapuruvu), presented a mannose/galactose (M/G) ratio of ~2.5, are abundant throughout Brazilian forests and could be an additional source of galactomannan for biotechnological applications. This galactomannan is similar to a galactomannan widely used in the pharmaceutical industry, obtained from the seeds of the locust bean gum, which presents a M/G ratio of ~3.5 (Bresolin, Milas, Rinaudo, & Ganter, 1998; Ganter, Heyraud, Petkowicz, Rinaudo, & Reicher, 1995). The M/G ratio depends on the source and method of extraction (Bento et al., 2013; Salvallagio, Freitas, Franquetto, Koop, & Silveira, 2014).

Xanthan gum is an extracellular polysaccharide of *Xanthomonas campestris*. Its primary structure is a cellulose backbone of D-glucose linked β-1,4 and on every alternate glucose unit, there is a side chain consisting of β-D-mannose-(1,4)-β-D-glucuronic acid-(1,2)-α-D-mannose. The terminal mannose moiety may carry pyruvate residues linked to the 4- and 6-positions. The internal mannose unit is acetylated at *O*-6 (Jansson, Kenne, & Lindberg, 1975). Xanthan solutions exhibit weak gel-like properties at low shear rates, making it suitable as a suspending agent; it does not gel at any concentration or temperature (Dea et al., 1977; Milas, Rinaudo, & Tinland, 1985). Xanthan has the remarkable feature of forming physical hydrogels when mixed with galactomannans, *e.g.* locust bean gum in 1:1. The formation involves synergistic interactions between these polysaccharides (Richter, Brand, & Berger, 2005; Sandolo, Coviello, Matricardi, & Alhaique, 2007). Examples of current applications of xanthan and the locustbean gum are drug delivery tablet systems, commercially known as TIMERx®, developed by Penwest Pharmaceuticals Company (Baichwall & Neville,

* Corresponding author. Tel.: +55 41 3361 1665; fax: +55 41 3360 5330.
E-mail addresses: jlms12@yahoo.com, jlms12@ufpr.br (J.L.M. Silveira).

http://dx.doi.org/10.1016/j.carbpol.2014.07.043
0144-8617/

2002), which in the presence of dextrose (50%) form a strong binder gel in water. The function of xanthan in tablets is to erode or dissolve slowly and thereby yield a more delayed release of active ingredients, compared to formulations devoid of hydrocolloids (McCall & Baichwall, 1994).

Xanthan and galactomannan from the seeds of *Mimosa scabrella* form a hydrogel matrix, studied to improve the stability of ascorbic acid in pharmaceutical formulations (Koop, Praes, Reicher, Petkowicz, & Silveira, 2009). Recently, a hydrogel made from CUR/xanthan and galactomannan from the seeds of *Ceratonia siliqua* (locust bean gum) was investigated by the authors (Da-Lozzo et al., 2013; Koop et al., 2012). We determine its rheological properties as well as its biocompatibility using the chorioallantoic membrane from *Gallus domesticus*. This binary system could be an alternative for hydrophobic compounds, such as CUR, which showed therapeutic effects on wound healing and protection against the deleterious effects of UVA-induced skin cancers injury by attenuating oxidative stress and suppressing inflammation upon topical application (Heng, 2010; Huang et al., 1997; Santibáñez, Quintanilla, & Martinez, 2000).

CUR is a low molecular weight polyphenol extracted from the rhizomes of turmeric (*Curcuma longa* Linn.). It has the chemical structure [1,7-bis(4-hydroxy-3-methoxyphenyl)hepta-1,6-diene-3,5-dione] and is water-insoluble. CUR is widely used in traditional Chinese medicine and in its food industry (Ammon & Wahl, 1991). It has additionally demonstrated several types of biological and pharmacological activities, including anti-inflammatory and antioxidant properties. However, previous studies have shown that the retention time of CUR in the body is limited due to its rapid systemic elimination (Kurd et al., 2008; Yang, Huang, & Lin, 2007).

The percutaneous route may be suitable for the administration of CUR for both local and systemic therapeutic uses. To enhance its bioavailability, the technique of encapsulation or incorporation with different polymers have been employed, including chitosan (Sanoj Rejinold et al., 2011), cyclodextrin (Tomren, Másson, Loftsson, & Tønnesen, 2007), methoxy poly(ethylene glycol)-graft-chitosan film (Li, Nan, Li, Zhang, & Chen, 2012b), nanocomposite of *N*,*O*-carboxymethylchitosan and oxidized alginate (Li et al., 2012a), and poly(ethyleneglycol)-poly(ε-caprolactone)-poly(ethyleneglycol) hydrogel (Gong et al., 2013). Previously we develop a lecithin-based CUR-containing microemulsion. However, the CUR mobility was thereby facilitated through the most external skin layers, including the stratum corneum (Koop et al., 2012).

In the present work, we proposed a strategy for cutaneous wound healing, which combined a CUR-loaded microemulsion (MC) without ethanol with an *in situ* gel-forming hydrogel system of xanthan and galactomannan from *S. parahybae* (XGMC). Furthermore, the stability, rheological properties, *in vitro* drug release, skin permeation and *in vivo* anti-inflammatory effect were determined to investigate the topical effects on cutaneous wound models.

2. Materials and methods

2.1. Chemicals and reagents

CUR powder (89.5% purity), isopropyl myristate and egg L-α-phosphatidylcholine were purchased from Sigma-Aldrich Co. (Steinheim, GER). Benzylic alcohol and xanthan (X) were obtained from Merck (Darmstadt, GER). Polysorbate 80 (Tween 80), 1,2-propanediol and phosphoric acid were obtained from Synth (São Paulo, Brazil). Water was purified using Easy Pure equipment, with resistivity above 18 MΩ cm (Barnstead/Thermo scientific, Waltham, USA). The other chemicals are of HPLC or analytical grade.

Seeds from *S. parahybae* (guapuruvu) were acquired from *Viveiro Mata Atlântica*, São Paulo. The galactomannan was extracted from the isolated endosperm of guapuruvu seeds (G) using water at 25 °C for 1 h with mechanical stirring; the extract was centrifuged at 1,680 × *g* for 30 min at 10 °C (yield 42.1%). The supernatant was precipitated by adding ethanol and dried under vacuum (Bresolin et al., 1997). The M/G ratio of the galactomannan of G, determined by alditol acetate derivatization, was 2.5 (Wolfrom & Thompson, 1963a,b). Size exclusion chromatography (SEC) was carried out as described by Vianna-Filho, Petkowicz, and Silveira (2013); the average molar mass was 7.73×10^5 g mol^{-1} for the G, and the recovered mass from the system was 91.5% at 25 °C, suggesting good solubility in this aqueous solvent.

2.2. Preparation and characterization of the microemulsion

The MC was obtained by the method described previously (Lin, Lin, Chen, Yu, & Lee, 2009) with minor modifications. Oil (0.6 g), lecithin (0.765 g), Tween 80 (1.785 g), and CUR (0.09 g) were added in a test tube. The oil phase (isopropyl myristate) was kept at 50 °C and well mixed by a vortex. Water (15 g) was added with constant agitation, after sonication until a transparent mixture, an isotropic O/W MC, was obtained. The average hydrodynamic diameters (D_h) of the oil droplets were determined by dynamic light scattering in a BI 9000 multiangle laser light-scattering apparatus from Brookhaven Instruments (Holtsville, NY, USA). MC stability was assessed as a function of temperature. The samples were analyzed by DLS—Nano DLS Brookhaven Instruments (Holtsville, NY, USA) between 25 °C and 60 °C at a fixed angle of 90°. All measurements were performed at 25 °C in triplicate.

2.3. Preparation of hydrogels

Hydrogels were used as CUR vehicles in the *in-vivo* and *in-vitro* studies. The hydrogel formulations were prepared with X and G. In the first formulation (XG), X and G (50% of both) were dispersed in distilled water for 16 h at 1.25% total polysaccharide concentration in the presence of 1% benzyl alcohol (w/w) as a preservative and were used as a control without CUR. In the second formulation (XGMC), the MC was added to the XG hydrogel to compare the influence of MC on the hydrogel structure and to observe whether the MC preparation facilitates the "entrapment" of drug, such that the drug is not released. In the third formulation (XGEC), CUR was solubilized in ethanol (EC) and added 7.6 mL to 100 g of XG hydrogel, this amount was experimentally defined to not precipitate the polysaccharides. All samples were stirred for 10 min at room temperature, and all hydrogels were stored at 4 °C.

2.4. Stability and incorporation efficiency of curcumin-loaded hydrogel

The stability of the hydrogels was evaluated to verify that their chemical stability was maintained and that the following aspects of each active ingredient of the product was maintained: (a) the chemical integrity; (b) CUR concentration within the specified limits; (c) constant CUR concentration during storage and use; and (d) the properties and characteristics of the product (Isaac et al., 2008).

XG, XGEC and XGMC hydrogel samples were placed into a sealed glass bottle and in an oven at 45.0 ± 0.2 °C for 45 days. The samples were withdrawn 1, 15, 30 and 45 days after preparation. The stability was confirmed by centrifugation (Sigma 2K15, Osterode am Harz, Germany) at 1,107 × *g* at 25 °C for 30 min. The pH of the hydrogels was determined by using digital pH meter, directly in the sample, but promoting rupture of the gel structure by stirring, and measuring in different parts the samples. Additionally, we compare the pH of one gram of gel dissolved in 10 mL distilled water and stored for 30 min prior to measurement. The measurement of pH of each formulation was done in triplicate and average values are

Table 1
Hydrogel evaluation after 24 h and 45 days of storage at 45 °C.

Sample	Polymer (g %)	*IE*[a] (%)	*DC*[b] 45 days (%)	pH initial	pH 45 days
XGEC	1.25	96.9	96.9	5.2	5.0
XGMC	1.25	103.9	98.6	5.3	5.1

[a] *IE*—incorporation efficiency.
[b] *DC*—drug content.

calculated. The pH was measured at 25 °C (pHmeter Quimis, Diadema, SP, Brasil) and the rheology measurements were performed (Section 2.5).

The incorporation efficiency (*IE*) of CUR was determined by high-performance liquid chromatography (HPLC) according to the validated method of CUR quantification described by Koop, Freitas, Souza, and Silveira (2013). The concentration of CUR in the MC was determined as the mass ratio between the amount of CUR incorporated in the MC or the hydrogel-MC and the quantity used for preparation:

$$IE = \left(\frac{M}{M_T}\right) \times 100 \quad (1)$$

where M is CUR mass incorporated as determined by HPLC and M_T is CUR theoretical mass in the XGEC or XGMC.

The maintenance of drug content (*DC*) in the XGEC or XGMC was determined using the following equation:

$$DC = \frac{(IE \times M)}{100} \quad (2)$$

The color, odor and pH of the hydrogels were evaluated; no differences were observed in the saffron yellow color of the hydrogels, and the characteristic smell of CUR remained the same after 45 days. As presented in Table 1, a slight decrease of the pH of the hydrogels was observed after storage at 45 °C, indicating the stability of the formulation. The pH was 5.2–5.3 at the beginning of the experiment, and after 45 days, it was recorded at 5.0 and 5.1 for XGEC and XGMC, respectively. The centrifugation of the samples demonstrated physical stability and an absence of phase separation or material deposition.

The *IE* of the CUR in the hydrogels was evaluated using HPLC as described previously (Section 2.4). The experimental quantity of CUR content within the hydrogels was found to be close to the theoretical content, with a 5% deviation (Table 1). After 45 days, the CUR content of XGMC decreased to 98.6%; however, this variation of incorporated CUR fell within the specifications of drug degradation for pharmaceutical preparations (González, Herrador, & Asuero, 1999).

2.5. Rheological measurements

Dynamic oscillatory measurements were performed using a dynamic stress rheometer RS75 (Haake, Karlsruhe, Germany) equipped with cone and plate geometry (60 mm diameter, 2° cone angle, and 0.105 mm gap). The temperature was controlled by a circulating water bath and regulated by a Peltier effect at 25 °C. Prior to the frequency sweep analysis the deformation oscillatory experiments by stress sweeps at a constant frequency (1 Hz) were performed. They were done to determine the linear viscoelastic range of the samples. The measured stress value was then used for the frequency sweeps, and they were conducted under constant strain in the field of linear viscoelasticity. The strain amplitude chosen was 1%. Further rheological measurements were executed as described by Koop et al. (2012). All tests were replicated at least three times; mean values and corresponding standard errors were calculated.

2.6. In vitro drug release from hydrogels

The *in vitro* drug release from the hydrogels was analyzed using a dialysis cellulose ester membrane (cut off 6000–8000 g mol^{-1}, Spectra/Por CE; Spectrum Laboratories, Rancho Dominguez, California), previously wetted for 12 h with the dissolution medium composed of buffered phosphate pH 7.4, 15% 1,2-propanediol, 5% HPLC grade ethanol, and 1% Tween 80 (v/v). Free CUR or hydrogels, corresponding to 60 mg of CUR were placed into the dialysis membrane and suspended into the dissolution medium. The system was rotated (150 rpm) at 37 ± 0.5 °C. The samples (1 mL) were withdrawn every hour, for 10 h, with the replacement of the dissolution medium (Shaikh, Ankola, Beniwal, Singh, & Kumar, 2009). The CUR concentrations were determined by HPLC.

A mathematical model describes the release of drugs from swellable polymeric systems. The model was employed to fit the data for the preliminary evaluation of the release of CUR from the binary hydrogel using the following equation:

$$\text{First order}: \frac{M_t}{M_\infty} = 1 - \exp(-k_1 t) \quad (3)$$

where M_t is the CUR mass released, M_∞ is the total CUR mass released from the propylene glycol solution, k_1 is the release constant and t is time in hours.

2.7. In-vitro skin permeation

The full-thickness of porcine ear skin was used for the permeation experiments. Porcine-ears were collected immediately after the slaughter of Large White male pigs, aged approximately 6 months and approximately 90 kg (Frigorífico Frigomug, Brazil). The skin was clamped between the donor and the receptor chamber of a vertical diffusion cell with an effective diffusion area of 2.8 cm^2 and a 6.7-mL cell volume (Microette Apparatus, Hanson Research, Chatsworth, USA). The receptor chamber was filled with fresh dissolution medium (Section 2.6). The diffusion cell was maintained in occlusive conditions at 37 °C using a re-circulating water bath, and the solution in the receptor chambers was stirred continuously at 300 rpm. The formulation (1.0 g) was gently placed in the donor chamber. From 2 to 18 h, 1.0 mL of the solution in the acceptor chamber was removed for HPLC analysis and replaced immediately with an equal volume of dissolution medium. All experiments were performed in triplicate.

At the end of the study, the receptor fluid was removed and analyzed by HPLC. The Franz cells were dismantled, the skin layers were separated by stripping, and CUR was extracted with methanol. The samples were filtered and analyzed by HPLC according to the previously validated method (Koop et al., 2013).

2.8. Potential of reactivity/cutaneous irritation analysis

The reactivity or cutaneous irritation analysis was conducted for the semi-solid preparations containing CUR at a concentration of 0.6 mg g^{-1} (w/w) using agarose overlay or agar diffusion tests (Invittox, 1990; United States Pharmacopeial Convention, 2009) to evaluate the sample reactivity with L929 cells. This assay distinguishes metabolically active cells from injured and dead cells. The experiments were performed in triplicate, and the data are reported as the mean ± S.D. Statistical analysis was performed using GraphPad Instat software, version 3.05 (GraphPad Software, San Diego, California). The values were analyzed using one-way analysis of variance followed by the Tukey multiple-comparisons test. *P* values of <0.05 were considered significant.

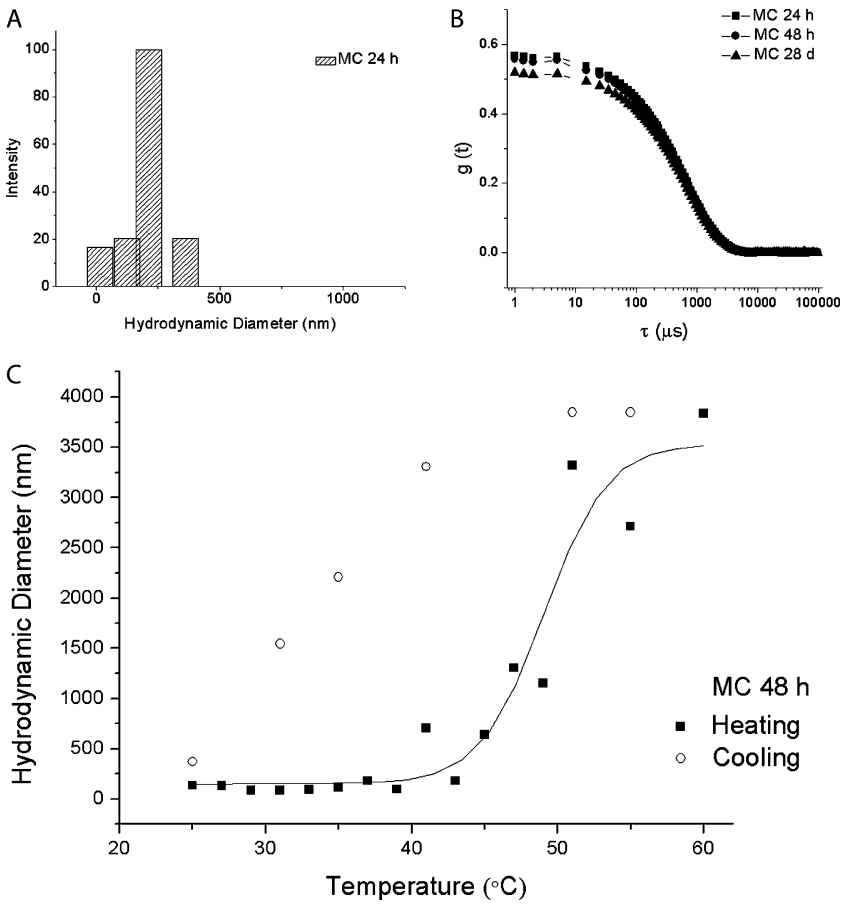

Fig. 1. (A) Size distribution of curcumin microemulsion after 24 h of preparation. (B) Correlation time of curcumin microemulsions determined by DLS at different times of preparation: (■) after 24 h, (●) after 48 h, (▲) after 28 days. (C) Hydrodynamic diameter of curcumin microemulsion after 48 h of preparation, during heating and cooling process.

2.9. Evaluation of anti-inflammatory effects in vivo by croton oil-induced mouse ear edema

The *in vivo* evaluation of XG (vehicle), XGEC and XGMC hydrogels was performed using male Swiss mice (25–35 g) that were kept in a temperature-controlled environment (22 °C) on a 12 h light/dark cycle, with free access to food and water, except during the experiments. The procedures in these animals were performed in accordance with the protocol approved by the ethics committee in research from UNIVALI under the number 018/2009.

The topical anti-inflammatory effect was evaluated according to the croton oil-induced ear edema method described previously (Zanini, Medeiros, Cruz, Yunes, & Calixto, 1992), with minor modifications. The animals were divided into four different groups ($n = 10$). The right ear was measured (basal measure), and croton oil (2.5% v/v in acetone) was applied, as an irritating agent, to the external surface. Thirty minutes later, the following hydrogels (100 mg) were applied to the internal surface: the gel without CUR (negative control), ointments containing dexamethasone 0.5% (w/w) as a positive control, and the hydrogel samples containing CUR. Six hours after the administration of the oil, the ears were measured again, and the ear edema was evaluated using the difference between the two measurements (expressed in mm).

The results were expressed as the mean ± S.D. For the group comparisons, one-way layout analysis of variance was applied. The data were analyzed statistically using variance analysis followed by Dunnett's multiple comparison test. *P* values of <0.01 were considered significant.

3. Results and discussion

The poor water solubility and stability of CUR greatly limit its *in vivo* applications. To overcome these shortcomings, MCs were prepared. The combination of non-ionic surfactants with lecithin is very effective and gives optimal reproducibility to the system.

3.1. Microemulsion properties

The MCs were transparent with a saffron yellow color and remained clear up to 4 weeks. MC has characteristics of microemulsion (Lin et al., 2009), the apparent hydrodynamic diameter of the oil nanodroplets (D_h, nm) had a narrow monomodal distribution, with a mean value of 231.8 ± 7.6 nm (Fig. 1A), within the upper limit for the size for microemulsions and with isotropicity and stability over time (Fig. 1B). The autocorrelation functions obtained had a constant degree of decay as a function of storage time; according to these functions, the macromolecular structure was maintained.

The stability of the MCs was studied before incorporated them into the binary hydrogel. After one month of storage, there was no change in clarity or phase separation. The CUR concentration remained at 0.5% evaluated by HPLC, and over 99.5% of the drug was incorporated into the nanodroplets, according validated method (Koop et al., 2013).

The size temperature dependence (from 25 °C to 60 °C) of the MCs was also determined by DLS. Upon heating the MCs to 45 °C, an increase in MC particle size was observed, indicating particle fusion or aggregation. However, upon cooling of the sample, restructuring

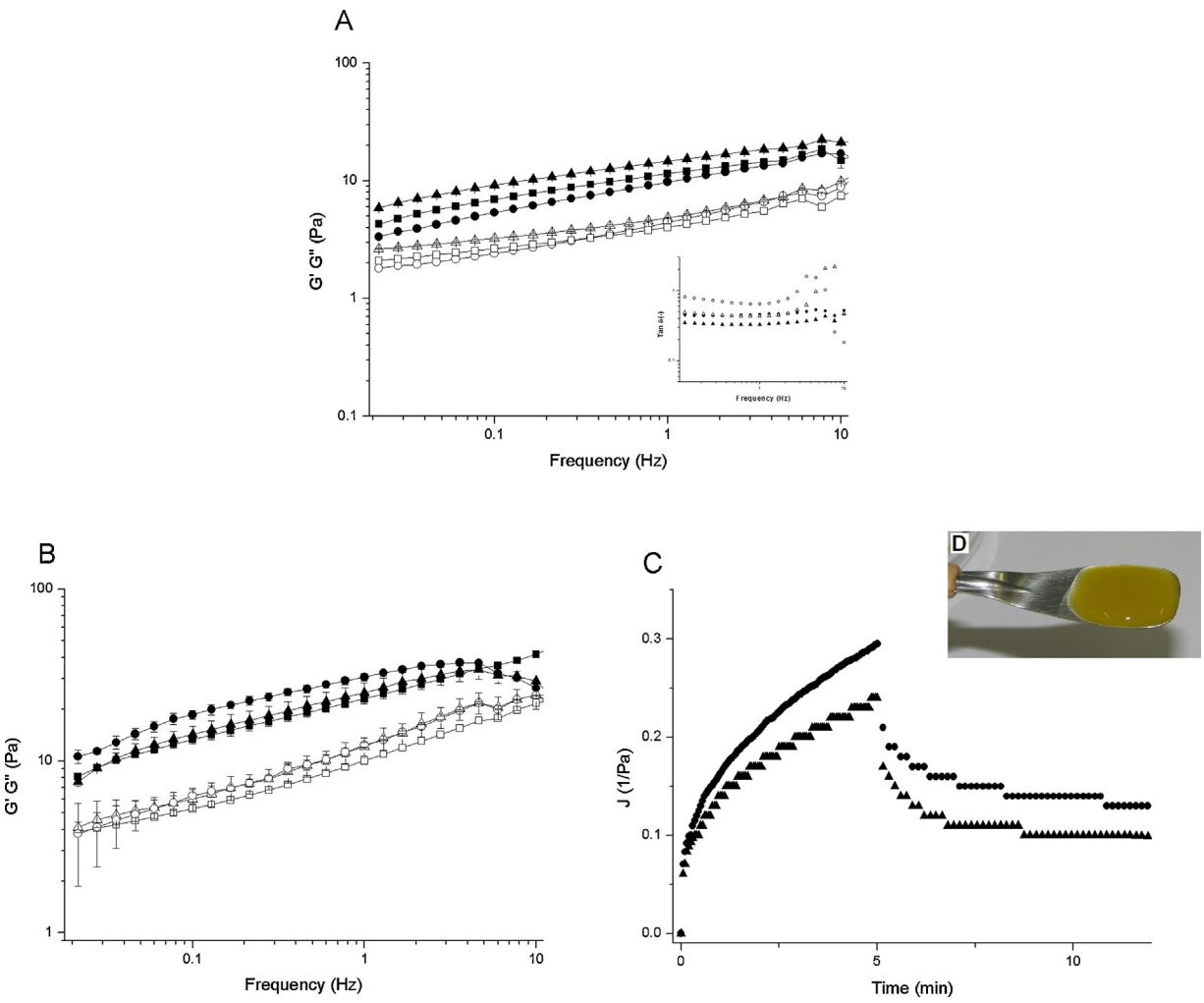

Fig. 2. (A) Frequency dependence of G' and G'' of xanthan–galactomannan hydrogels at 25 °C. The strain amplitude was set to 1%. Key: XG (■), XGEC (▲), XGMC (●); filled and open symbols represent G' and G'', respectively. Inset: Plot of tan δ obtained from the frequency sweep analysis from 0.1 to 10 Hz, at 25 °C. Key: XGEC (▲), XGMC (●); filled and open symbols represent values obtained after 1 and 45 days, respectively. (B) Frequency dependence of G' and G'' of xanthan–galactomannan hydrogels at 32 °C. (C) Xanthan–galactomannan hydrogel compliance *versus* time in the "creep and recovery" test. Measurements were performed at 25 °C with a constant stress of 0.5 Pa in the creep phase. Key: XGEC (▲), XGMC (●); filled and open symbols represent G' and G'', respectively. (D) Photo of XGMC.

of the MC occurred, and the light scattering intensity was similar from the beginning of the experiment (Fig. 1C).

The oil phase chosen for MC preparation was isopropyl myristate that had a CUR solubility of 0.03 wt%. The MC had a thermal stability up to 60 °C, and the D_h indicated stability for 28 days.

3.2. Rheological properties of the hydrogels

Fig. 2A shows the mechanical spectra of XG, XGEC and XGMC one day after the preparation of the hydrogels at 25 °C. All samples presented a gel behavior; both moduli had a slight frequency dependence, with G' (dynamic elastic or storage modulus) exceeding G'' (dynamic viscous or loss modulus) at all frequencies. The three hydrogels showed G' approximately 10 Pa at 1 Hz. Our early studies (Koop et al., 2012) showed that hydrogels obtained with X and the galactomannan of the locust bean gum with the addition of MC presented a G' of 438 Pa at 1 Hz. The lower value of G' for XGMC, is related to the difference in the M/G ratio of the galactomannan, which is ~3.5 for the locust bean gum, thus rendering higher interactions with the xanthan chains than with the galactomannan of *S. parahybae* (M/G of 2.5).

The tan δ values of XGEC and XGMC one day after preparation of the hydrogel were 0.3 and 0.5, respectively, at 1 Hz (inset-Fig. 2A). After the stability evaluation (45 days after preparation, Section 2.4), the tan δ values increased to 0.4 and 0.6 for XGEC and XGMC, respectively. The increase of tan δ values (value being close to 0 is indicative of a gel behavior and close to 1 is indicative of a more "liquid"-like behavior) of XGEC and XGMC 45 days after preparation of the hydrogel are characteristic of a weak gel (Schramm, 2000).

The hydrogels were also evaluated by oscillatory rheometry at 32 °C, so as to represent the temperature of skin (Fig. 2B). All three hydrogels remained as gels and showed both moduli having a slight frequency dependence, with G' exceeding G'' at all frequencies.

The viscoelastic behavior and a correlation of the primary skin feel with the rheological properties can be also evaluated using creep and recovery tests. Fig. 2C shows the creep and recovery curves for the XGEC and XGMC hydrogels; each profile is characteristic of a viscoelastic gel. During the creep and recovery phases, the hydrogel samples presented an instant and similar elastic response (J_o = 0.19 and 0.21 Pa for XGEC and XGMC, respectively). The lower the value of J_o, greater the elasticity is. Some permanent viscous deformation was observed after stress removal at the recovery phase (J_r = 52.2 and 49.6%, for XGEC and XGMC, respectively). J_r represents the "elastic recovery" immediately after the stress is removed. These results demonstrated a similar viscoelastic behavior for both hydrogels.

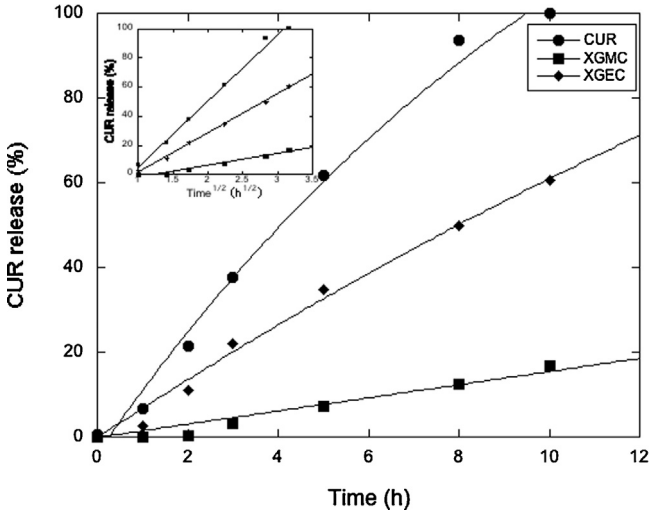

Fig. 3. Release profile of curcumin from the hydrogels in phosphate solution at 150 rpm and 37 ± 0.5 °C. Inset: Graphic according Higuchi's plot. Key: CUR solution in propylene glycol (●); XGEC (■), XGMC (▲).

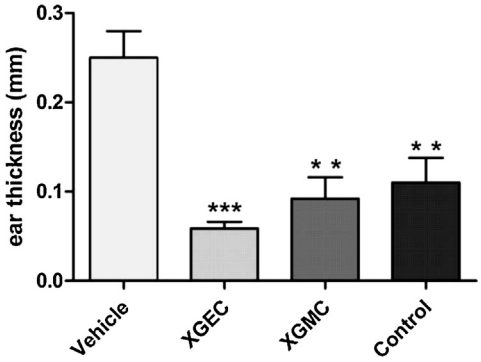

Fig. 4. Anti-inflammatory activity of the hydrogels with curcumin (XGEC and XGMC). The vehicle is the XG hydrogel, and the control is an ointment containing dexamethasone 0.5% (w/w). The data represent the mean ± S.D. of 10 mice. The statistical significance of ear thickness was analyzed using variance analysis following Dunnett's multiple comparison test; ** $p < 0.01$; *** $p < 0.001$.

The mechanical spectra obtained for XGMC and XGEC (Fig. 2A–D) demonstrated the elastic behavior of the gels and the presence of a cross-linked intermolecular structure of the polysaccharides, which were maintained even after 45 days at 45 °C.

3.3. *In vitro drug release study*

The *in vitro* release profiles of CUR from binary hydrogels are presented in Fig. 3, showing a sustained liberation of CUR over 10 h. This profile was consistent with a first order kinetic profile, with a dissolution value of $k = 1.1 \times 10^{-4}\ h^{-1}$ for XGMC. The release profile of CUR from XGEC ($k = 2.9 \times 10^{-2}\ h^{-1}$) was similar to that of the CUR solution in propylene glycol ($k = 5.9 \times 10^{-2}\ h^{-1}$).

The amount of CUR released (%) from the gel formulation *versus* the square root of time (inset-Fig. 3) represents the CUR release, except in the lag phase up to 1 h, where no release was measured. From 1 to 10 h, according to the Higuchi plot (Higuchi, 1963) for a drug delivery <60%, a diffusion-controlled mechanism of CUR release from the hydrogels was observed. An excellent linear relationship was observed (>0.99) for all samples using the Higuchi plot.

3.4. *In-vitro skin permeation*

The *in vitro* skin permeation analysis revealed similar quantities of CUR in the three layers of the skin: stratum corneum, epidermis and dermis. As shown in Table 2, the CUR concentrations were found to be 2.15 to 2.50 μg mL^{-1}. In the reception fluid of the diffusion cells, no quantities of CUR were determined, most likely due to a higher affinity of the drug to the superficial layers of the skin and due to the characteristics of the MCs (O/W with D_h of 231.8 nm). According to Teichmann et al. (2007), lipid layers and follicles seem to be the preferred pathways for the penetration of lipophilic drugs, as indicated by microscopic observations, and nanoparticles can modulate the delivery of active substances and residence time in the skin (Beck, Guterres, & Pohlmann, 2011).

The percutaneous absorption of CUR across rat skin treated with enhancers from solutions and carboxymethyl cellulose–Na^+–hydrogels was examined by Fang, Hung, Chiu, Wang, and Chan (2003). The enhancers significantly increased the passive absorption of CUR by the skin. Terpineol increased the flux of CUR 4.15-fold relative to the control, but they exhibited some toxicity according to skin histology and trans-epidermal water loss experiments.

Table 2
Curcumin penetration in the entire porcine ear membrane.

Hydrogels	Stratum corneum (μg mL^{-1})	Epidermis (μg mL^{-1})	Dermis (μg mL^{-1})
XGEC	2.30 ± 0.28	2.15 ± 0.07	2.20 ± 0.00
XGMC	2.45 ± 0.25	2.17 ± 0.05	2.47 ± 0.09

Reported as means of triplicates (±S.D.).

3.5. *Potential of reactivity/cutaneous irritation analysis (mucous membrane irritation test)*

To determine whether nanoparticles interfere with the activity of CUR when in contact with living cells, an *in vitro* reactivity experiment using an agarose overlay was adopted for assaying XG (vehicle), XGEC and XGMC hydrogels. The results showed no reactivity for free CUR, for CUR solubilized in propylene glycol and for the two hydrogels tested. The *in vitro* agarose overlay method is an alternative to the Draize test for the ranking of ocular irritancy of detergent-based products. It is useful as a screening assay in irritancy prediction by evaluating the incorporation of the vital dye neutral red by viable cells (O'Brien, Jones, & Rockley, 1990; Horan, Clotworthy, Fokunang, & Tomkins, 2003).

3.6. *In vivo anti-inflammatory test*

The *in vivo* evaluation of anti-inflammatory effects was determined for XG (vehicle), XGEC and XGMC hydrogels. Fig. 4 shows the animal test results of the anti-inflammatory activity of CUR incorporated in the hydrogels. The incorporation of CUR into XG hydrogels did not influence its intrinsic antioxidant efficiency and anti-inflammatory activity, as demonstrated by edema inhibition on mouse ear. The maximal inhibition of inflammation was 76.8% for XGEC, and XGMC presented 63.2% inhibition. Compared with dexamethasone 0.5% (w/w) as a positive control, the inhibition was higher for CUR-loaded hydrogels. Gong et al. (2013) studied composites of thermosensitive PEG-poly(ε-caprolactone)-PEG hydrogel loaded with CUR; these polymers exhibited wound-healing activity in rats. The authors suggested that a combination of the bioactivity of CUR and the thermosensitive hydrogel promoted the tissue reconstruction processes.

4. Conclusions

XGEC and XGMC obtained with the galactomannan extracted from the seeds of the Brazilian native tree *S. parahybae* (guapuruvu) were used for the preparation of binary hydrogels. These hydrogels have the potential to meet some of the challenges involved in hydrophobic drug nanoformulations for topical application. These composites have a high drug encapsulation efficiency of 99.5%, a first order kinetic profile of drug release and *in vitro* skin permeation revealed up to 2.50 $\mu g\,mL^{-1}$ of CUR in the skin layers. CUR showed a slow release (XGMC) compared to the release profiles for the CUR solution in propylene glycol, which may be attributed to the incorporation of CUR into the microemulsion. For effective topical use, the rheological properties of XGEC and XGMC allowed for prolonged exposure over the skin during the treatment, offering long-lasting action and, a potential target to treat skin diseases such as skin cancer and psoriasis. The hydrogels are safe because no cutaneous membrane irritation was found from *in vitro* cytotoxicity tests and because they presented up to 76.8% inhibition of inflammation on mouse ear, higher than the positive control of the method; thus, these hydrogels hold great potential in the delivery of hydrophobic drugs in general.

Acknowledgements

The authors thank the following Brazilian funding agencies for financial support: National Research Council of Brazil (CNPq no. 476950/2013-9), the Araucaria Foundation (PRONEX-Carboidratos, no. 117/2010), Nanoglicobiotec-Ministry of Science and Technology/CNPq no. 564741/2010-8, and the Federal University of Paraná-Brazil. J.L.M.S. and R.A.F. are research members of the CNPq (no. 306949/2012-1). H.S.K. is the beneficiary of a post-doctoral scholarship from Nanoglicobiotec-Ministry of Science and Technology/CNPq no. 564741/2010-8.

References

Ammon, H., & Wahl, M. A. (1991). Pharmacology of *Curcuma longa*. *Planta Medica*, *57*, 1–7.

Baichwall, A., & Neville, D. A. (2002). Culturing innovation and enhancing medications using oral drug delivery. *Drug Delivery Technology*, *2*, 65–68.

Beck, R., Guterres, S., & Pohlmann, A. (2011). Nanocosmetics and nanomedicines: New approaches for skin care. In N. Durán, Z. Teixeira, & P. D. Marcato (Eds.), *Topical application of nanostructures* (pp. 69–99). Berlin Heidelberg: Springer-Verlag.

Bento, J. F., Mazzaro, I., Silva, L. M. de A., Moreira, R. A., Ferreira, M. L. C., Reicher, F., & Petkowicz, C. L. O. (2013). Diverse patterns of cell wall mannan/galactomannan occurrence in seeds of the Leguminosae. *Carbohydrate Polymers*, *92*, 192–199.

Bresolin, T. M. B., Sander, P. C., Reicher, F., Sierakowski, M. R., Rinaudo, M., & Ganter, J. L. M. S. (1997). Viscometric studies on xanthan and galactomannan systems. *Carbohydrate Polymers*, *33*, 131–138.

Bresolin, T. M. B., Milas, M., Rinaudo, M., & Ganter, J. L. M. S. (1998). Xanthan–galactomannan interactions as related to xanthan conformations. *International Journal of Biological Macromolecules*, *23*, 263–275.

Da-Lozzo, E. J., Moledo, R. C. A., Faraco, C. D., Ortolani-Machado, C. F., Bresolin, T. M. B., & Silveira, J. L. M. (2013). Curcumin/xanthan–galactomannan hydrogels: Rheological analysis and biocompatibility. *Carbohydrate Polymers*, *93*, 279–284.

Dea, I. C. M., Morris, E. R., Rees, D. A., Welsh, E. J., Barnes, H. A., & Price, J. (1977). Associations of like and unlike polysaccharides: Mechanism and specificity in galactomannans, interacting bacterial polysaccharides, and related systems. *Carbohydrate Research*, *57*, 249–272.

Fang, J. Y., Hung, C. F., Chiu, H. C., Wang, J. J., & Chan, T. F. (2003). Efficacy and irritancy of enhancers on the *in-vitro* and *in-vivo* percutaneous absorption of curcumin. *Journal of Pharmacy and Pharmacology*, *55*, 593–601.

Ganter, J. L. M. S., Heyraud, A., Petkowicz, C. L. O., Rinaudo, M., & Reicher, F. (1995). Galactomannans from Brazilian seeds: Characterization of the oligosaccharides produced by mild acid hydrolysis. *International Journal of Biological Macromolecules*, *17*, 13–19.

Gong, C. Y., Wu, Q. J., Wang, Y. J., Zhang, D. D., Luo, F., Zhao, X., Wei, Y. Q., & Qian, Z. Y. (2013). A biodegradable hydrogel system containing curcumin encapsulated in micelles for cutaneous wound healing. *Biomaterials*, *34*, 6377–6387.

González, A., Herrador, M. A., & Asuero, A. G. (1999). Intra-laboratory testing of method accuracy from recovery assays. *Talanta*, *48*, 729–736.

Heng, M. C. Y. (2010). Curcumin targeted signaling pathways: Basis for anti-photoaging and anti-carcinogenic therapy. *International Journal of Dermatology*, *49*, 608–622.

Higuchi, T. (1963). Mechanism of sustained-action medication. *Journal of Pharmaceutical Science*, *52*, 1145–1149.

Horan, I., Clotworthy, M., Fokunang, C. N., & Tomkins, P. T. (2003). The development of an *in vitro* screening strategy for topically applied products. *Journal of Ethnopharmacology*, *89*, 81–90.

Huang, M. T., Ma, W., Yen, P., Xie, J. G., Han, J., Frenkel, K., Grunberger, D., & Conney, A. H. (1997). Inhibitory effects of topical application of low doses of curcumin on 12-*O*-tetradecanoylphorbol-13-acetate-induced tumor promotion and oxidized DNA bases in mouse epidermis. *Carcinogenesis*, *18*, 83–88.

Invittox. (1990). *Ergatt-frame. Agarose overlay assay 1990 protocol 31*.

Isaac, V. L. B., Cefali, L. C., Chiari, B. G., Oliveira, C. C. L. G., Salgado, H. R. N., & Corrêa, M. A. (2008). Protocolo para ensaios físico-químicos de estabilidade de fitocosméticos. *Revista de Ciências Farmacêuticas Básica e Aplicada*, *29*, 81–96.

Jansson, P.-E., Kenne, L., & Lindberg, B. (1975). Structure of the extracellular polysaccharide from *Xanthomonas campestris*. *Carbohydrate Research*, *45*, 275–282.

Koop, H. S., Praes, C. E. O., Reicher, F., Petkowicz, C. L. O., & Silveira, J. L. M. (2009). Rheological behavior of gel of xanthan with seed galactomannan: Effect of hydroalcoholic–ascorbic acid. *Materials Science and Engineering C*, *29*, 559–563.

Koop, H. S., Da Lozzo, E. J., Franco, C. R. C., Martinez, G. R., Mitchell, D. A., & Silveira, J. L. M. (2012). Rheological characterization of a xanthan–galactomannan hydrogel loaded with lipophilic substances. *Journal of Pharmaceutical Sciences*, *101*, 2457–2467.

Koop, H. S., Freitas, R. A. de., Souza, L. M., & Silveira, J. L. M. (2013). Stability-indicating LC–PDA method for determination of curcuminoids in microemulsions and polysaccharide hydrogel. *Chromatographia*, *76*, 1041–1048.

Kurd, S. K., Smith, N., Voorhees, A. V., Troxel, A. B., Badmaev, V., Seykora, J. T., & Gelfand, J. M. (2008). Oral curcumin in the treatment of moderate to severe psoriasis vulgaris: A prospective clinical trial. *Journal of American Academy of Dermatology*, *58*, 625–631.

Li, X., Chen, S., Zhang, B., Li, M., Diao, K., Zhang, Z., Li, J., Xu, Y., Wang, X., & Chen, H. (2012). In situ injectable nano-composite hydrogel composed of curcumin, *N*,*O*-carboxymethyl chitosan and oxidized alginate for wound healing application. *International Journal of Pharmaceutics*, *437*, 110–119.

Li, X., Nan, K., Li, L., Zhang, Z., & Chen, H. (2012). In vivo evaluation of curcumin nanoformulation loaded methoxypoly(ethyleneglycol)-graft–chitosan composite film for wound healing application. *Carbohydrate Polymers*, *88*, 84–90.

Lin, C.-C., Lin, H.-Y., Chen, H.-C., Yu, M.-W., & Lee, M.-H. (2009). Stability and characterisation of phospholipid-based curcumin-encapsulated microemulsions. *Food Chemistry*, *116*, 923–928.

Mannion, R. O., Melia, C. D., Launay, B., Cuvelier, G., Hill, S. E., Harding, S. E., & Mitchell, J. R. (1992). Xanthan/locust bean gum interactions at room temperature. *Carbohydrate Polymers*, *19*, 91–97.

McCall, T. W., & Baichwall, A. R. (1994). In vitro–*in vivo* correlation of TIMERx–metoprolol products. In *Proceedings of the international symposium controlled release bioactive materials, Vol. 21* (pp. 812–813).

Milas, M., Rinaudo, M., & Tinland, B. (1985). The viscosity dependence on concentration, molecular weight and shear rate of xanthan solutions. *Polymer Bulletin*, *14*, 157–164.

O'Brien, K. A. F., Jones, P. A., & Rockley, J. (1990). Evaluation of an agarose overlay assay to determine the eye irritation potential of detergent-based products. *Toxicology in Vitro*, *4*, 311–313.

Richter, S., Brand, T., & Berger, S. (2005). Gelation studies, 3 comparative monitoring of the gelation process of a thermoreversible gelling system made of xanthan gum and locust bean gum by dynamic light scattering and ^{1}H NMR spectroscopy. *Macromolecular Rapid Communications*, *26*, 548–553.

Salvallagio, M. O., Freitas, R. A., Franquetto, E. M., Koop, H. S., & Silveira, J. L. M. (2014). Influence of the extraction time on macromolecular parameters of galactomannans. *Carbohydrate Polymers*, http://dx.doi.org/10.1016/j.carbpol.2014.05.036 (in press)

Sandolo, C., Coviello, T., Matricardi, P., & Alhaique, F. (2007). Characterization of polysaccharide hydrogels for modified drug delivery. *European Biophysics Journal*, *36*, 693–700.

Sanoj Rejinold, N., Muthunarayanan, M., Divyarani, V. V., Sreerekha, P. R., Chennazhi, K. P., Nair, S. V., Tamura, H., & Jayakumar, R. (2011). Curcumin-loaded biocompatible thermoresponsive polymeric nanoparticles for cancer drug delivery. *Journal of Colloid and Interface Science*, *36*, 39–51.

Santibáñez, J. F., Quintanilla, M., & Martinez, J. (2000). Genistein and curcumin block TGF-β_1-induced u-PA expression and migratory and invasive phenotype in mouse epidermal keratinocytes. *Nutrition and Cancer*, *37*, 49–54.

Schramm, G. (2000). The measurement of the elastic behavior of visco-elastic fluids. In *A practical approach to rheology and rheometry* (2nd ed., pp. 121–133). Karlsruhe: Gebrueder Haake GmbH.

Shaikh, A., Ankola, D. D., Beniwal, V., Singh, D., & Kumar, M. N. (2009). Nanoparticle encapsulation improves oral bioavailability of curcumin by at least 9-fold when compared to curcumin administered with piperine as absorption enhancer. *European Journal of Pharmaceutical Science*, *37*, 223–230.

Teichmann, A., Heuschkel, S., Jacobi, U., Presse, G., Neubert, R. H. H., Sterry, W., & Lademann, J. (2007). Comparison of stratum corneum penetration and localization of a lipophilic model drug applied in an o/w microemulsion and an amphiphilic cream. *European Journal of Pharmaceutics and Biopharmaceutics*, *67*, 699–706.

Tomren, M. A., Másson, M., Loftsson, T., & Tønnesen, H. H. (2007). Studies on curcumin and curcuminoids XXXI. Symmetric and asymmetric curcuminoids:

Stability, activity and complexation with cyclodextrin. *International Journal of Pharmaceutics*, *338*, 27–34.
Ughini, F., Andreazza, I. F., Ganter, J. L. M. S., & Bresolin, T. M. B. (2004). Evaluation of xanthan and highly substituted galactomannan from *M. scabrella* as a sustained release matrix. *International Journal of Pharmaceutics*, *271*, 197–205.
United States Pharmacopeial Convention. (2009). *United States pharmacopeia* (29th ed.). Rockville: United States Pharmacopeial Convention.
Vendruscolo, C. W., Andreazza, I. F., Ganter, J. L. M. S., Ferrero, C., & Bresolin, T. M. B. (2005). Xanthan and galactomannan (from *M. scabrella*) matrix tablets for oral controlled delivery of theophylline. *International Journal of Pharmaceutics*, *296*, 1–11.
Vianna-Filho, R. P., Petkowicz, C. L. O., & Silveira, J. L. M. (2013). Rheological characterization of O/W emulsions incorporated with neutral and charged polysaccharides. *Carbohydrate Polymers*, *93*, 266–272.
Wolfrom, M. L., & Thompson, A. (1963a). Reduction with sodium borohydride. *Methods of Carbohydrate Chemistry*, *2*, 65–68.
Wolfrom, M. L., & Thompson, A. (1963b). Acetylation. *Methods of Carbohydrate Chemistry*, *2*, 211–215.
Yang, C. H., Huang, K. S., & Lin, Y. C. (2007). Using a cross-flow microfluidic chip and external crosslinking reaction for monodisperse TPP-chitosan microparticle. *Sensors and actuators B: Chemical*, *124*, 510–516.
Zanini, J. C., Medeiros, Y. S., Cruz, A. B., Yunes, R. A., & Calixto, J. B. (1992). Action of compounds from *Mandevilla velutina* on croton oil-induced ear edema in mice. A comparative study with steroidal and nonsteroidal antiinflammatory drugs. *Phytotherapy Research*, *6*, 1–5.